NATIONAL AERONAUTICS AND SPACE ADMINISTRATION

Technical Report No. 32-789

Similarity in Confined Vortex Flows

E. J. Roschke
T. J. Pivirotto

JET PROPULSION LABORATORY
CALIFORNIA INSTITUTE OF TECHNOLOGY
PASADENA, CALIFORNIA

August 15, 1965

NATIONAL AERONAUTICS AND SPACE ADMINISTRATION

Technical Report No. 32-789

Similarity in Confined Vortex Flows

E. J. Roschke
T. J. Pivirotto

D. R. Bartz, *Manager*
Research and Advanced Concepts Section

JET PROPULSION LABORATORY
CALIFORNIA INSTITUTE OF TECHNOLOGY
PASADENA, CALIFORNIA

August 15, 1965

Prepared Under Contract No. NAS 7-100
National Aeronautics & Space Administration

CONTENTS

TABLES

FIGURES

ABSTRACT

Results of an experimental investigation designed to test a simplified theory for obtaining dynamic similarity in confined vortex flows are presented. The simplified model from which similarity is obtained consists of the vortex flow of dissimilar fluids under conditions of exact geometric similarity. Steady, laminar, viscous, compressible flow in a two-dimensional, axisymmetric vortex is considered. The experiment consists of end-wall pressure measurements using the two diatomic gases, nitrogen and hydrogen, in identically the same vortex apparatus. Experiments were conducted using a cylindrical vortex tube 4.5-in. internal diameter and 24-in. long, having a 0.625-in. D exit hole or orifice centrally located in one end-wall, the other end of the vortex tube being closed. Approximately 800 tangential driving jets were used to initiate and maintain the vortex flow. The basis for judging similarity in separate experiments using nitrogen and hydrogen was comparison of the radial static-pressure distributions as measured at the closed end-wall of the vortex tube and normalized with respect to the static pressure at the cylindrical wall.

The results are discouraging from the standpoint of achieving dynamic flow similarity under the proposed theoretical model. It is concluded that the proposed model is too restrictive in that it neglects the effects of turbulence and axial velocities. However, since very little quantitative information on these factors exists for the vortex flows of present interest, they were necessarily eliminated from consideration. The results of this investigation thus tend to show that simplified theories of vortex flow are insufficient, but the degree or precise manner of their defect cannot be delineated.

Examination of another set of data using the identical vortex apparatus disclosed that dynamic similarity in static-pressure distributions (measured at the closed end-wall) between tests using nitrogen and hydrogen could be closely approached by conducting the tests at equal values of static pressure at the cylindrical wall. Some of the latter results are presented and discussed.

Author

I. INTRODUCTION

Knowledge which would enable an investigator to achieve dynamic similarity between two or more vortex flows would be extremely valuable because it would (a) permit the design of separate experiments for investigation of selected phenomena, and (b) indicate the conditions under which a comparison of the work of individual experimentalists would be valid. However, the specification of appropriate and tractable similarity rules requires a reasonably complete understanding of the flow field under consideration. Since confined vortex flows are not well understood, it appears almost hopeless to attempt such a problem. A first step in this direction might be to set up a simple rule or rules for similarity covering a very simple case and then test the validity of the result by experiment. The results of such an approach are presented here.

The model from which similarity was obtained consisted of the vortex flow of dissimilar fluids under conditions of exact geometric similarity. The experiment consisted of observations using the diatomic gases nitrogen and hydrogen in identically the same apparatus. For such a simple case, it would appear that similarity could be achieved through proper account of such fluid properties as viscosity, specific-heat ratio, thermal conductivity, and molecular weight. The experiment is termed simple merely because of the simplicity inherent in the test itself and not because the flow case studied is elementary.

The results were discouraging, since dynamic flow similarity was not achieved under the proposed model. However, even this negative result is somewhat instructive.

II. DEVELOPMENT OF SIMILARITY CONDITIONS

In the vortex flows of interest here (Fig. 1), it is believed that the radial component of fluid velocity is everywhere small compared with the tangential component, except within the end-wall boundary layers. However, the radial velocity component and its radial gradient are not necessarily negligible in all the equations of motion and are, therefore, retained as required in the following development. Although little is known concerning the axial velocity component, it appears likely that it is not negligible relative to the tangential component, particularly within the viscous-core region; i.e., in a region near the vortex axis. The model selected for this study is two-dimensional in character such that axial velocity and axial variations in all dependent flow variables are neglected. This assumption results in a simple, tractable model that may be tested experimentally; it is not justified on physical grounds. It is apparent from Fig. 1, for example, that the assumption $w = 0$ is not compatible with the existence of fluid leaving the vortex exit-hole, as shown. However, examination of the radial momentum equation in cylindrical coordinates indicates that axial variations in flow variables are small compared with the pressure term and radial acceleration terms. Consequently, in experimental work, the end-wall static-pressure distributions are thought to be practically independent of existing axial variations in the vortex flow field.

In classic studies of dynamic flow similarity, complete geometric similarity is usually considered a prerequisite. Geometric similarity between two objects is obtained when all linear dimensions of the two objects scale on a single, arbitrarily chosen, dimension. In this study, the vortex aspect ratio L/D and the relative exit-hole size d_0/D are considered to be the necessary conditions for geometric similarity. Necessary and sufficient conditions for geometric similarity would also include a statement concerning the fluid-injection geometry, which, however, is not considered here.

Laminar, viscous, compressible flow in a two-dimensional vortex is considered. The flow is steady and axisymmetric, and internal heat generation (volume release) and body forces are neglected. A fluid having constant properties, subject to zero heat transfer to or from the walls of the container, is specified. With $w = 0$, the axial momentum

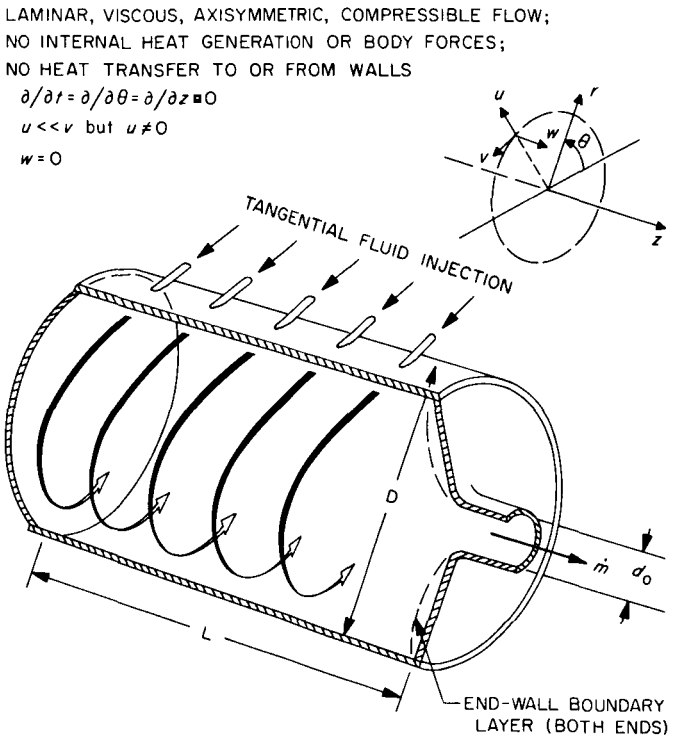

Fig. 1. Idealized vortex flow assumed for similarity model

equation vanishes, and with $\partial/\partial t = \partial/\partial\theta = \partial/\partial z = 0$, the remaining equations of continuity, momentum and energy become in cylindrical coordinates

$$\frac{1}{r}\frac{d(\rho u r)}{dr} = 0 \tag{1}$$

$$\rho u\left(\frac{dv}{dr} + \frac{v}{r}\right) = \mu\frac{d}{dr}\left(\frac{dv}{dr} - \frac{v}{r}\right) + \frac{2\mu}{r}\left(\frac{dv}{dr} - \frac{v}{r}\right) \tag{2}$$

$$\frac{dp}{dr} = \frac{\rho v^2}{r} - \rho u\frac{du}{dr} + \frac{4}{3}\mu\frac{d}{dr}\left(\frac{du}{dr} + \frac{u}{r}\right) \tag{3}$$

$$\rho u c_p\frac{dT}{dr} - u\frac{dp}{dr} = \frac{k}{r}\frac{d}{dr}\left(r\frac{dT}{dr}\right) + \Phi \tag{4}$$

where the dissipation function Φ in this case is given by

$$\Phi = \mu\left\{\left(\frac{dv}{dr} - \frac{v}{r}\right)^2 + \frac{4}{3}\left[\left(\frac{du}{dr}\right)^2 - \frac{u}{r}\frac{du}{dr} + \left(\frac{u}{r}\right)^2\right]\right\} \tag{5}$$

If $u^2 \ll v^2$, Eqs. 3 and 5 reduce to

$$\frac{dp}{dr} = \frac{\rho v^2}{r} \tag{6}$$

and

$$\Phi = \mu\left(\frac{dv}{dr} - \frac{v}{r}\right)^2 \tag{7}$$

Substitution of Eqs. 6 and 7 into Eq. 4 reduces the energy equation to

$$\rho u\left(c_p\frac{dT}{dr} - \frac{v^2}{r}\right) = \frac{k}{r}\frac{d}{dr}\left(r\frac{dT}{dr}\right) + \mu\left(\frac{dv}{dr} - \frac{v}{r}\right)^2 \tag{8}$$

Since $\rho u r$ = constant from Eq. 1 and u is negative in this problem, the usual definition for radial Reynolds number is adopted as follows,

$$Re_r = -\frac{\rho u r}{\mu} \tag{9}$$

or

$$Re_r = \frac{\dot{m}}{2\pi\mu L} \tag{10}$$

and Prandtl number is defined in the usual way, $Pr = \mu c_p/k$. Utilizing Eq. 9 and normalizing v,p and T with respect to their values at the cylindrical wall yields

$$r_* v_*'' + (Re_r + 1)\,v_*' + (Re_r - 1)\frac{v_*}{r_*} = 0 \tag{11}$$

$$p_*' = \frac{\rho_w v_w^2}{p_w}\frac{\rho_* v_*^2}{r_*} = \gamma M_w^2\frac{\rho_* v_*^2}{r_*} \tag{12}$$

$$T_*'' + \frac{(1 + Re_r Pr)}{r_*}T_*' = (\gamma - 1)\,Pr\,M_w^2\left[Re_r\left(\frac{v_*}{r_*}\right)^2 - \left(v_*' - \frac{v_*}{r_*}\right)^2\right] \tag{13}$$

where the prime denotes d/dr_* and the double prime denotes d^2/dr_*^2. Geometric similarity is prescribed. If, further, the appropriate boundary conditions for the problem are normalized with respect to values at the cylindrical wall and are prescribed similarly in two or more flows, then the solutions of Eqs. 11, 12, and 13 yield dynamic similarity of two flows in u, v, p and T when

$$(Re_r)_A = (Re_r)_B \tag{14}$$

$$(q_w/p_w)_A = (q_w/p_w)_B \text{ or } (M_w)_A = (M_w)_B \tag{15}$$

$$(\gamma)_A = (\gamma)_B \text{ and } (Pr)_A = (Pr)_B \tag{16}$$

Eq. 14 is the result of prescribing dynamic flow similarity when Eq. 11 is applied to two separate flows. In like manner, application of Eq. 12 results in Eq. 15 and application of Eqs. 11 and 13 result in Eq. 16. Note that

the requirements of Eq. 16 are automatically satisfied if similar flow of two diatomic (or two monatomic) gases is considered.

It is customary to consider the solutions of Eqs. 11, 12, and 13 in two portions, since strict application of Eq. 1 in the vortex core leads to a singularity at the axis where the fluid velocity becomes infinite. Depending on assumptions concerning the radial distribution of mass flow in the core (Ref. 1), Eqs. 11, 12, and 13 may be solved exactly or numerically.

It is well known from experimental work that values of Re_r computed from Eq. 10 and used in solutions of Eq. 11 do not yield tangential velocity profiles that compare favorably with those obtained experimentally. Reasonable comparison may be obtained only if an effective radial Reynolds number $Re_{r,e}$ much smaller than values given by Eq. 10 are used in solutions of Eq. 11. (See, for example, Refs. 1, 2 and 3.) The physical reasons for the discrepancy between $Re_{r,e}$ and Re_r are the subject of much conjecture (Refs. 2, 4, 5, and 6). However, despite the reasons for the discrepancy, it is much more realistic to use appropriate values of $Re_{r,e}$ in Eqs. 11, 12, and 13 than to use values of Re_r as defined by Eq. 10.

One method of predicting $Re_{r,e}$, based on radial mass-flow-rate depletion due to end-wall boundary-layer flow, is presented in Ref. 4 where it was found that

$$Re_{r,e} = Re_r - \frac{K(Re_t)^a}{L/D} \tag{17}$$

In Eq. 17, Re_t denotes the peripheral tangential Reynolds number equivalent to $\rho_w v_w D/2\mu$, and the term involving Re_t accounts for radial mass flow in two end-wall boundary layers. It is shown in Ref. 4 that Re_t is almost directly proportional to Re_r if the vortex driving jets are subsonic; the proportionality factor does not depend on the type of fluid. Re_r and Re_t are related through momentum change experienced by the driving fluid due to cylindrical wall-friction. The coefficient K is an amplitude function arising from assumptions concerning the radial velocity profile within the end-wall boundary layers and depends on radius, nature of the boundary-layer flow (laminar or turbulent), and the radial distribution of tangential velocity external to the boundary layers. The power a in Eq. 17 depends on whether the end-wall boundary layers are laminar or turbulent. The values of K and a will not be discussed further. Hopefully, in the experimental case to be described later, the values of K and a for one gas are the same as for the other gas so that their numerical values are unimportant. Thus, it appears that similarity will be achieved in two separate diatomic (or monatomic) gases when equivalence in $Re_{r,e}$ and M_w is maintained.

If equality in K, a and L/D exists between two separate vortex flows, use of Eq. 17 in the similarity model is still an admission of infinite similarity possibilities unless a relationship between Re_r and Re_t is known or specified. Without such a relationship, the simplest case that might be tested consists of imposing equality in Re_r, which then, through Eq. 17, also imposes equality in Re_t in two separate flows. For the latter case, the similarity conditions specified by Eqs. 14, 15 and 16 become

$$(Re_r)_A = (Re_r)_B \tag{18}$$

$$(Re_t)_A = (Re_t)_B \tag{19}$$

$$(q_w/p_w)_A = (q_w/p_w)_B \text{ or } (M_w)_A = (M_w)_B \tag{20}$$

$$(\gamma)_A = (\gamma)_B \text{ and } (Pr)_A = (Pr)_B \tag{21}$$

If a definite relationship between Re_r and Re_t is known or assumed (based on developments such as those outlined in Ref. 4), Eqs. 18 and 19 do not express independent requirements. In vortex apparatus of fixed configuration and dimensions, Re_t cannot be directly controlled, but is indirectly controlled through changes in $\dot{m}$ and hence Re_r. Therefore, it would be desirable to eliminate Re_t from requirements for experimental similarity tests. As shown in Ref. 4, the relationship between Re_r and Re_t is sufficiently near-linear that they may be considered directly proportional, for practical purposes. Hence, either of Eqs. 18 or 19 may be utilized, and equality in Re_r between two flows shall be considered equivalent to equality in $Re_{r,e}$ in those flows.

III. APPLICATION TO EXPERIMENT

Two gases, nitrogen and hydrogen, were tested separately in the vortex tube shown in Fig. 2 and described in Table 1. This vortex consisted of two concentric steel tubes, held together at both ends by flanges onto which end walls were bolted. The annular space between the tubes served as a supply manifold for each of the 804 driving-jet tubes, which were fabricated from 0.90-in. lengths of 0.062-in. OD × 0.007-in. ID stainless-steel tubing and cemented into holes drilled through the wall of the inner tube. The centerline of the jet tubes, arranged in a helix along the length of the vortex tube, were tangent to a circle with diameter 0.92, that of the vortex-tube diameter. The helix contained six jet orifices per revolution, which were distributed so as to cover the inner cylindrical surface of the tube. In all cases, the driving fluid passed through the jet orifices, thus generating a vortex flow, and was then discharged through the exit hole at the center of one end-wall.

A pitot tube and a bare-wire thermocouple were used to measure the fluid stagnation pressure and temperature upstream of a choked venturi, which was used to measure the mass rate of flow $\dot{m}$ delivered to the manifold. The manifold pressure and temperature and the static pressure at the cylindrical wall of the vortex were measured and recorded for each experimental run. The radial static-pressure distribution on the closed end-wall was measured with a pressure tap located in a circular disk built into the end-wall, as shown in Fig. 2. By rotating this disk, the static pressure at any radial position from the centerline to a point 0.127 in. from the cylindrical surface of the vortex tube could be determined.

Exact geometric similarity, including the injection system and exhaust configuration, was preserved. From Eqs. 19 and 20, and the equation of state for a perfect gas, the following relation for static wall pressure is obtained when $Re_r \propto Re_t$:

$$\frac{(p_w)_A}{(p_w)_B} = \frac{(\mu)_A}{(\mu)_B}\frac{(D)_B}{(D)_A}\left[\frac{(\mathcal{M})_B}{(\mathcal{M})_A}\frac{(T_w)_A}{(T_w)_B}\right]^{1/2} \tag{22}$$

In conducting the experiment, it became more convenient to use the inlet stagnation temperature, which was directly measured, rather than T. Since, in addition, $D_A = D_B$, the working form of Eq. 22 used to test the similarity model was

$$\frac{(p_w)_A}{(p_w)_B} = \frac{(\mu)_A}{(\mu)_B}\left[\frac{(\mathcal{M})_B}{(\mathcal{M})_A}\frac{(T_t)_A}{(T_t)_B}\right]^{1/2} \tag{23}$$

Near room temperature, Eq. 23 yields a ratio of static wall pressures, hydrogen to nitrogen, of approximately 2.0.

In an experiment, nitrogen was first run at a preselected value of p_w, and then a separate run was made using hydrogen at a value of p_w obtained from Eq. 23. An attempt was made to compensate for differing fluid temperature. In each case, the radial distribution of static pressure was measured at the closed end-wall. Mach number distributions were obtained by graphical differentiation of the measured pressure distributions and computed according to the relation

$$M = \left[\frac{r}{\gamma p}\frac{dp}{dr}\right]^{1/2} \tag{24}$$

These two parameters, (*i*) the radial distribution of static pressure normalized with respect to the wall value p_w, and (*ii*) the Mach number distribution, were used to judge the validity of the similarity model; they are not independent results, however.

Table 1. Principal dimensions of vortex tube[a]

Item	Symbol	Value
Vortex length	L	24 in.
Vortex diameter	D	4.5 in.
Aspect ratio	L/D	5.33
Exit-hole diameter	d_o	0.625 in.
Relative exit-hole diameter	d_o/D	0.139
Number of driving jets	—	804
Jet diameter	—	0.007 in.
Approximate aspect ratio of jets	—	130

[a]See also Fig. 2

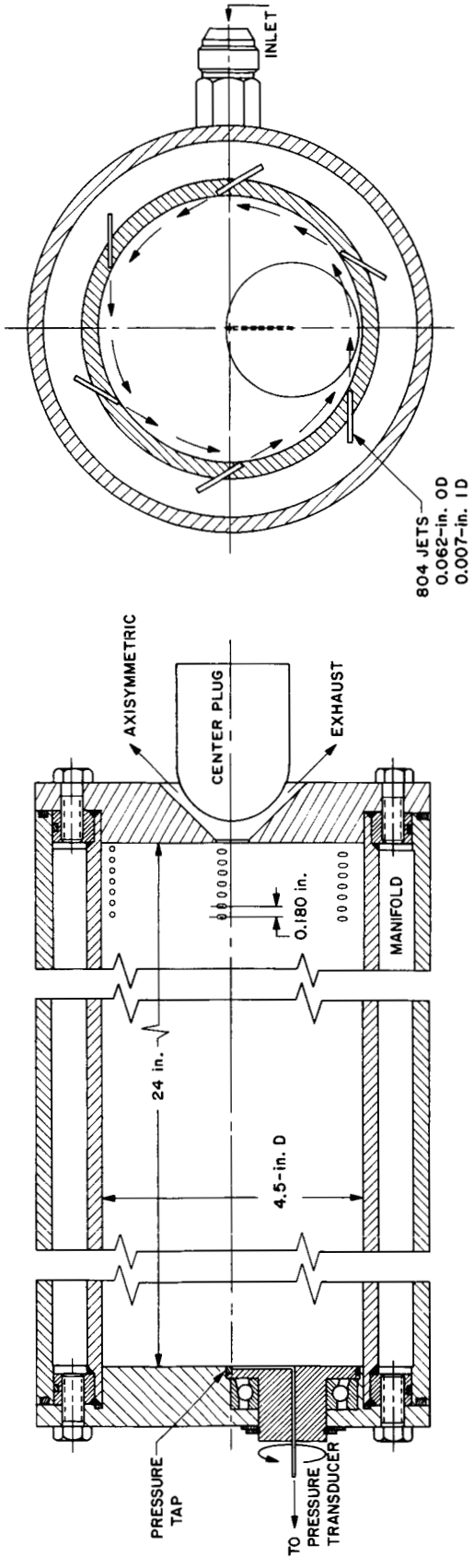

Fig. 2. Vortex tube

IV. EXPERIMENTAL RESULTS

Run pairs, using hydrogen and nitrogen under the similarity condition expressed by Eq. 23, were made at three separate levels of wall pressure. For convenience, these pressure levels shall be called low, medium, and high. A summary of the pertinent, measured and derived results are given in Tables 2(a) and 2(b), respectively. For example, runs A-1 and B-1 constitute a similarity pair. Runs B-4 and B-5 were additional runs, using nitrogen at wall pressures higher than in the similarity runs; they were not part of the similarity test and were obtained

Table 2. Experimental conditions for similarity run pairs

Item	Symbol	Type of gas and run designation							
		H_2	N_2	H_2	N_2	H_2	N_2	N_2	N_2
		A-1	B-1	A-2	B-2	A-3	B-3	B-4	B-5
(a) Measured conditions									
Mass flow rate, lb/sec	$\dot{m}$	0.0246	0.0333	0.0339	0.0607	0.0463	0.0910	0.1062	0.1290
Stagnation pressure (manifold or plenum), psia	P_{tm}	209.7	75.2	291.2	134.2	389.2	199.2	231.2	280.2
Static pressure at cylindrical wall, psia	P_w	38.7	20.2	54.2	28.2	74.2	38.2	44.2	54.2
Pressure ratio	P_w/P_{tm}	0.1842	0.282	0.1861	0.210	0.1907	0.1917	0.1913	0.1933
Ambient pressure, psia	P_a	14.19	14.19	14.19	14.19	14.19	14.19	14.19	14.19
Stagnation temperature (manifold or plenum), °R	T_{tm}	537	518	538	513	528	499	500	501
Ambient temperature, °R	T_a	522	520	525	523	521	520	521	522
Similarity condition	$\frac{(P_w)_A}{(P_w)_B}$	1.915		1.921		1.942		——	
(b) Computation from measured conditions									
Tangential Mach Number at wall[a]	M_w	0.17	0.16	0.175	0.17	0.18	0.185	0.19	0.195
Static temperature at cylindrical wall, °R[b]	T_w	534	515	533	507	525	496	496	497
Tangential velocity at wall, ft/sec	v_w	733	181	754	190	770	207	211	217
Radial Reynolds number	Re_r	329	239	456	435	624	651	761	925
Peripheral tangential Reynolds number[c]	Re_t	3.16×10^5	3.13×10^5	4.56×10^5	4.675×10^5	6.47×10^5	6.98×10^5	8.27×10^5	10.45×10^5
Reynolds number ratio $= \lvert u\rvert_w/v_w$	$\frac{Re_r}{Re_t}$	1.04×10^{-3}	0.764×10^{-3}	1.0×10^{-3}	0.93×10^{-3}	0.963×10^{-3}	0.932×10^{-3}	0.92×10^{-3}	0.88×10^{-3}
Similarity condition[d]	$\frac{(P_w)_A}{(P_w)_B}$	2.03		2.04		2.05		——	

[a]Computed from Eq. 24; dp/dr determined graphically.

[b]Determined from T_{tm} and M_w.

[c]Based on v_w.

[d]Computed from right side of Eq. 22.

merely for reference purposes. The similarity conditions expressed by $(p_w)_A/(p_w)_B$, given in Table 2(a) for the various tests, may be compared with their corresponding values listed in Table 2(b), which were computed using Eq. 22. Agreement is within 6%. Values for radial Reynolds number based on mass flow rate agree within 5% for the medium- and high-pressure run pairs (1 and 2), but disagree badly (by 38%) for the low-pressure case (3). Good agreement in M_w and Re_t was obtained for all similarity run pairs. Since M_w (and hence both v_w and Re_t) was obtained by graphical differentiation using the measured static pressure distributions, the accuracy of those values are not comparable to those of Re_r.

The static-pressure distributions and tangential Mach number distributions are shown for the three similarity cases in Figs. 3, 4 and 5. The curves for pressure distribution represent curves faired through many experimental points in each case; the individual points are not shown. In each of the figures, open and closed symbols (for nitrogen and hydrogen, respectively) denote values of tangential Mach number, computed as previously described, using Eq. 24.

In the low-pressure case (Fig. 3), very poor agreement in static pressure and, hence, Mach number, distributions was obtained. This may not be a crucial case, however,

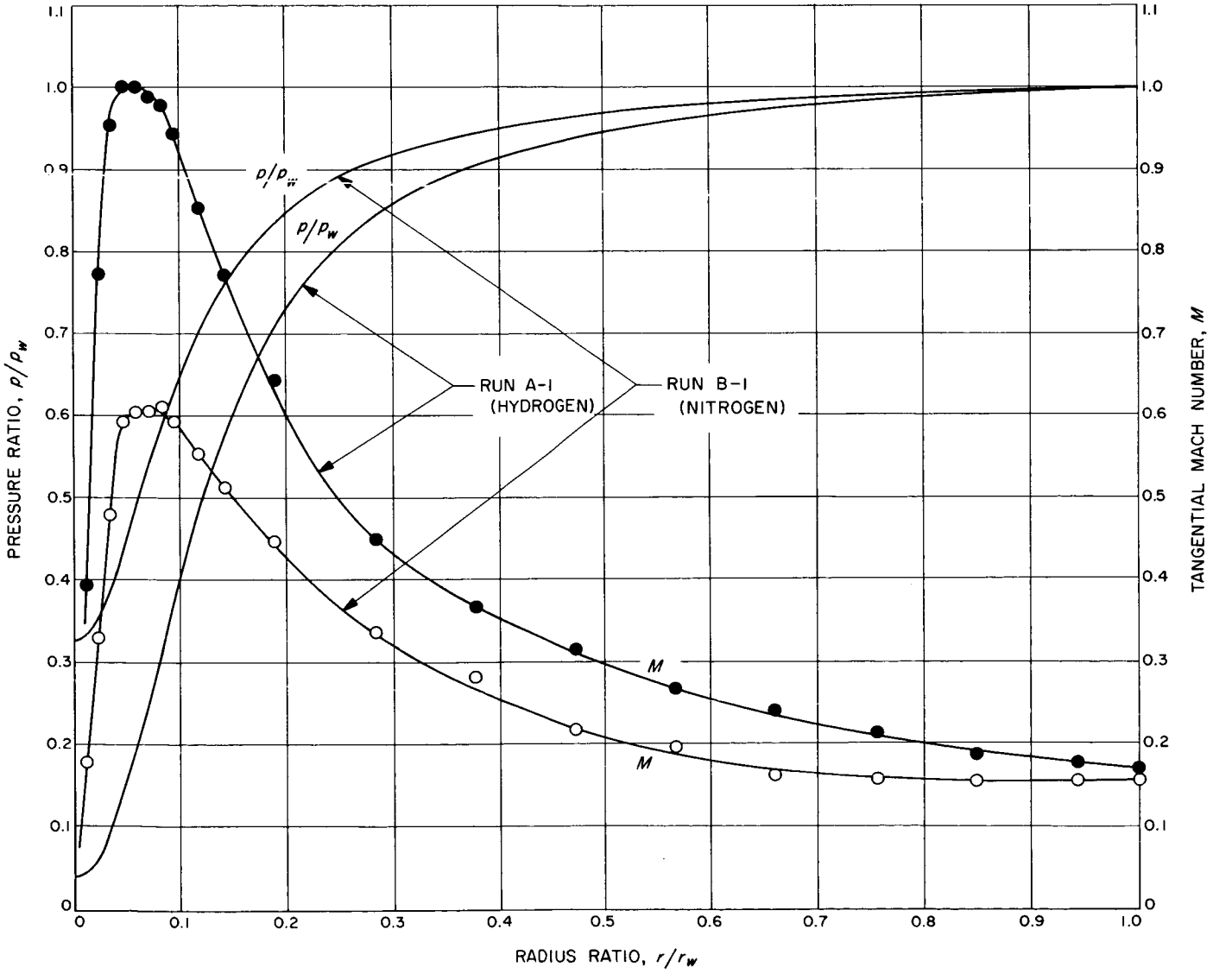

Fig. 3. Similarity test at low pressure

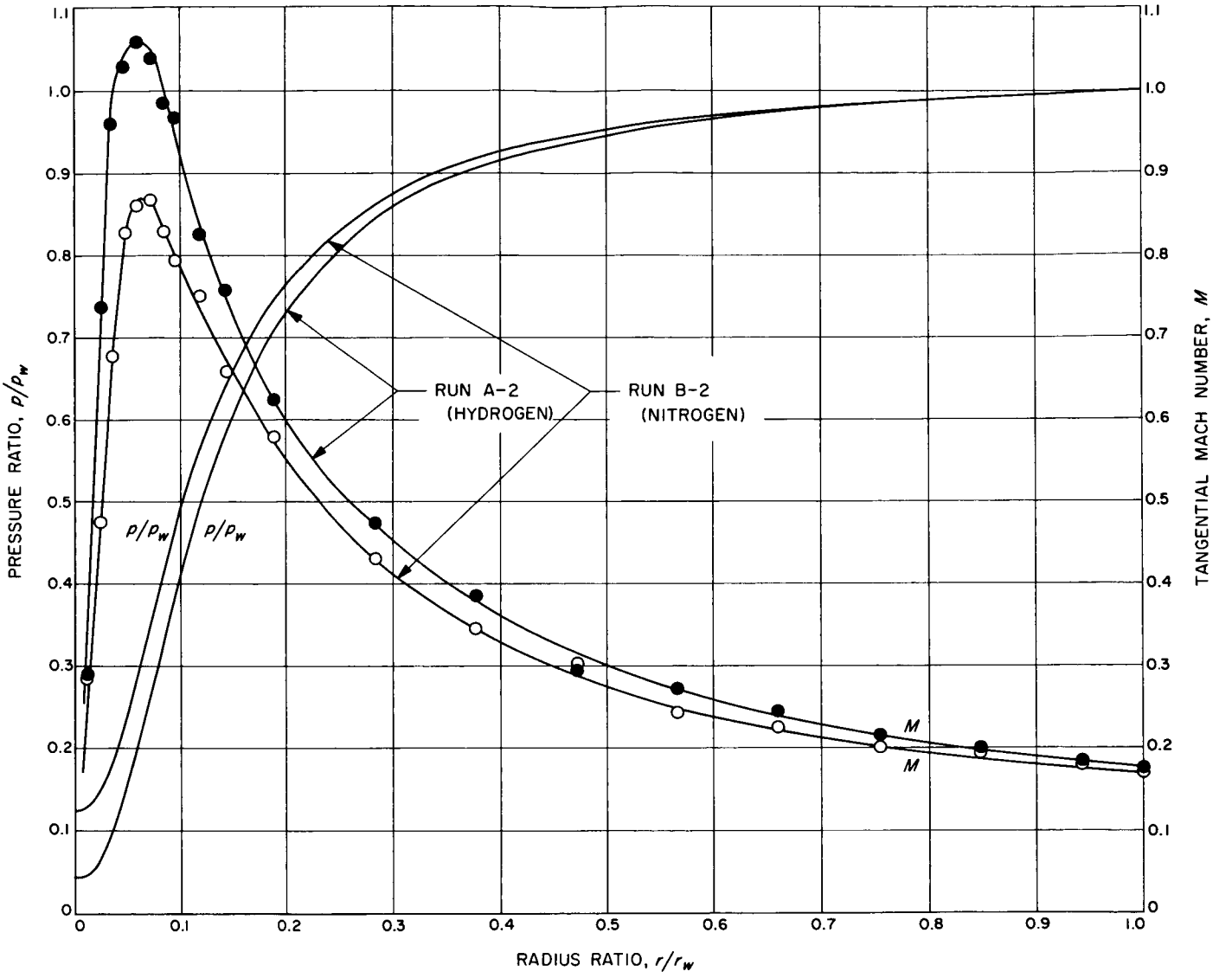

Fig. 4. Similarity test at medium pressure

since not all conditions imposed by the model were satisfied; i.e., $(Re_r)_A \neq (Re_r)_B$. The medium-pressure case (Fig. 4) furnishes a better case for comparison, since all conditions required by the similarity model were met to good approximation. Although similarity in pressure and Mach number was improved somewhat compared with the low-pressure case, it is definitely far from satisfactory. As can be seen from Fig. 5, a high degree of similarity exists for the high-pressure case, in which the pressure distributions differ only slightly in a region near the vortex axis and cannot be distinguished from one another throughout most of the vortex. The consistency of the slope technique for determining Mach number may be assessed by examining Fig. 5. Although some scatter is apparent when comparing values denoted by the open and closed symbols, the Mach number distributions are essentially the same, as would be required by similarity in the pressure distributions.

It is not appropriate to assume that the similarity model proposed here is successful at an arbitrarily high-pressure level, such as depicted in Fig. 5. The apparent similarity in the latter case has no obvious connection with the similarity model. In fact, it was determined that the pressure distributions shown in Fig. 5, for runs A-3 and B-3, represent approximately a limiting pressure distribution for this vortex configuration. Pressure distributions obtained for runs B-4 and B-5 (not presented here) were almost identical with those shown in Fig. 5, differing only slightly in a region very near the vortex axis. This

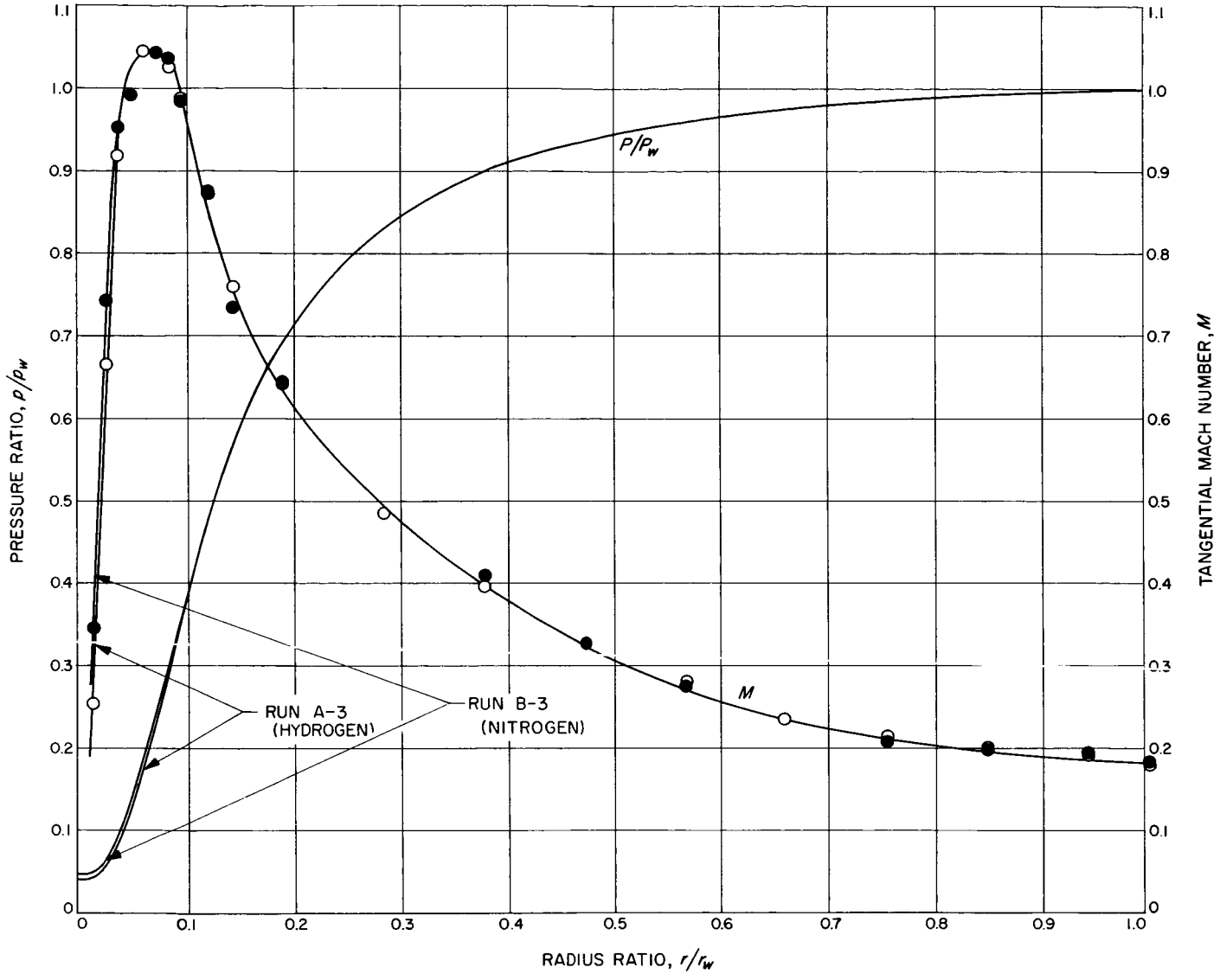

Fig. 5. Similarity test at high pressure

apparent limiting pressure distribution occurs in both hydrogen and nitrogen, but at different values of mass flow rate, which are, however, not sharply defined. Increasing $\dot{m}$ beyond those points produces very little change in the normalized distributions of static pressure, as measured at the closed end-wall, except near the vortex centerline. Thus, it appears likely that operation at any arbitrary values of $\dot{m}$ greater than that value required to produce the limiting case would produce similar static-pressure distributions in different diatomic gases.

At the highest values of $\dot{m}$ obtainable in this configuration, with exit-hole sizes smaller than those employed in the present study, there was some evidence to show that the peak value of tangential Mach number occurring in the vortex, increased with increasing $\dot{m}$, attained a maximum and then decreased slightly with further increases of $\dot{m}$. These data, which are insufficient to be considered general, would seem to indicate, at least for the smaller exit-hole sizes, that (a) a true limiting static-pressure distribution may not exist, but, rather (b) that an optimum pressure distribution (one having the maximum possible static pressure gradient and yielding a maximum possible tangential Mach number) may exist.

Examination of a different body of data, recorded for other purposes in identically the same apparatus, disclosed that a simple method of achieving a high degree of

Table 3. Summary of experimental conditions for run pairs having equal values of static wall pressure[a]

Item	Symbol	Type of gas and run designation									
		H_2	N_2	H_2	N_2	H_2	N_2	H_2	N_2	H_2	N_2
		A-6	B-6	A-7	B-7	A-8	B-8	A-9	B-9	A-10	B-10
		With 0.010-in Diameter Wire In Vortex						Without Wire			
Mass flow rate, lb/sec	$\dot{m}$	0.0085	0.0320	0.0171	0.0630	0.0440	0.1640	0.0420	0.1510	0.0530	0.1910
Stagnation pressure (manifold or plenum), psia	P_{tm}	70.8	72.5	146.0	139.5	367	351	352	330	433	413
Static pressure at cylindrical wall, psia	P_w	19.4		29.0		71.6		77.4		96.7	
Pressure ratio	P_w/P_{tm}	0.273	0.267	0.1985	0.208	0.195	0.204	0.220	0.234	0.223	0.234
Stagnation temperature (manifold or plenum) °R	T_{tm}	539	533	552	525	525	483	517	512	510	504
Radial Reynolds number ratio	$\frac{(Re_r)_B}{(Re_r)_A}$	2.015		1.958		1.984		1.915		1.920	

[a]Ambient conditions, pressure and temperature, similar to values shown in Table 2.

similarity in static-pressure distributions between hydrogen and nitrogen did exist. Similarity in the end-wall static-pressure distributions, except at very low $\dot{m}$, was obtained simply by conducting tests (using the two gases separately) at the same value of static wall pressure p_w. Some of the experimental conditions for these tests are given in Table 3, and the results are shown, for various pressure levels, in Figs. 6 and 7. The vortex configuration was the same as described previously (Table 1 and Fig. 2).

Before elaborating on Figs. 6 and 7, it is necessary to point out that the test results appearing in Fig. 6 were obtained when a small probe-wire was stretched across a diameter of the vortex tube, whereas the results of Fig. 7 were obtained without the wire. The purpose of this wire is of no importance here; however, its presence modifies the relations between p_w, $\dot{m}$, and M_w somewhat, so that data taken with and without the wire should not be compared directly. Information on the purpose, use, and effects of small probe-wires on the vortex flow are contained in Ref. 7. Since, when using hydrogen as compared to nitrogen, differences in wire effects were not discernible, the data within Fig. 6 is valid and run-pairs may be compared. The same remark applies to Fig. 7.

Pairs of pressure distributions at three different values of p_w are shown in Fig. 6. The degree of similarity exhibited is very good, with the exception of run-pair A-6 and B-6, which agree, however, much better than do runs A-1 and B-1. The effect of the wire is partially demonstrated by comparing runs B-6 and B-1, which have comparable values of $\dot{m}$ and p_w. Referring to Fig. 7 (high-pressure runs obtained without a probe-wire), similarity between the pressure distributions of runs A-9 and B-9 is very good, whereas similarity between runs A-10 and B-10 is somewhat poorer. It is interesting to note that at the higher values of static wall-pressure tested, an increase in p_w (e.g., A-9 to A-10, or B-9 to B-10) produces a rise rather than a decrease in the normalized pressure at the vortex centerline. This result tends to confirm partially the remarks made earlier concerning a possible optimum pressure distribution.

In general, the results shown in Figs. 6 and 7 indicate that when hydrogen and nitrogen were run separately in this vortex-tube configuration at the same values of p_w, nitrogen consistently produced lower static pressures throughout the radial extent of the vortex away from the cylindrical wall. An exception occurred in the run pair

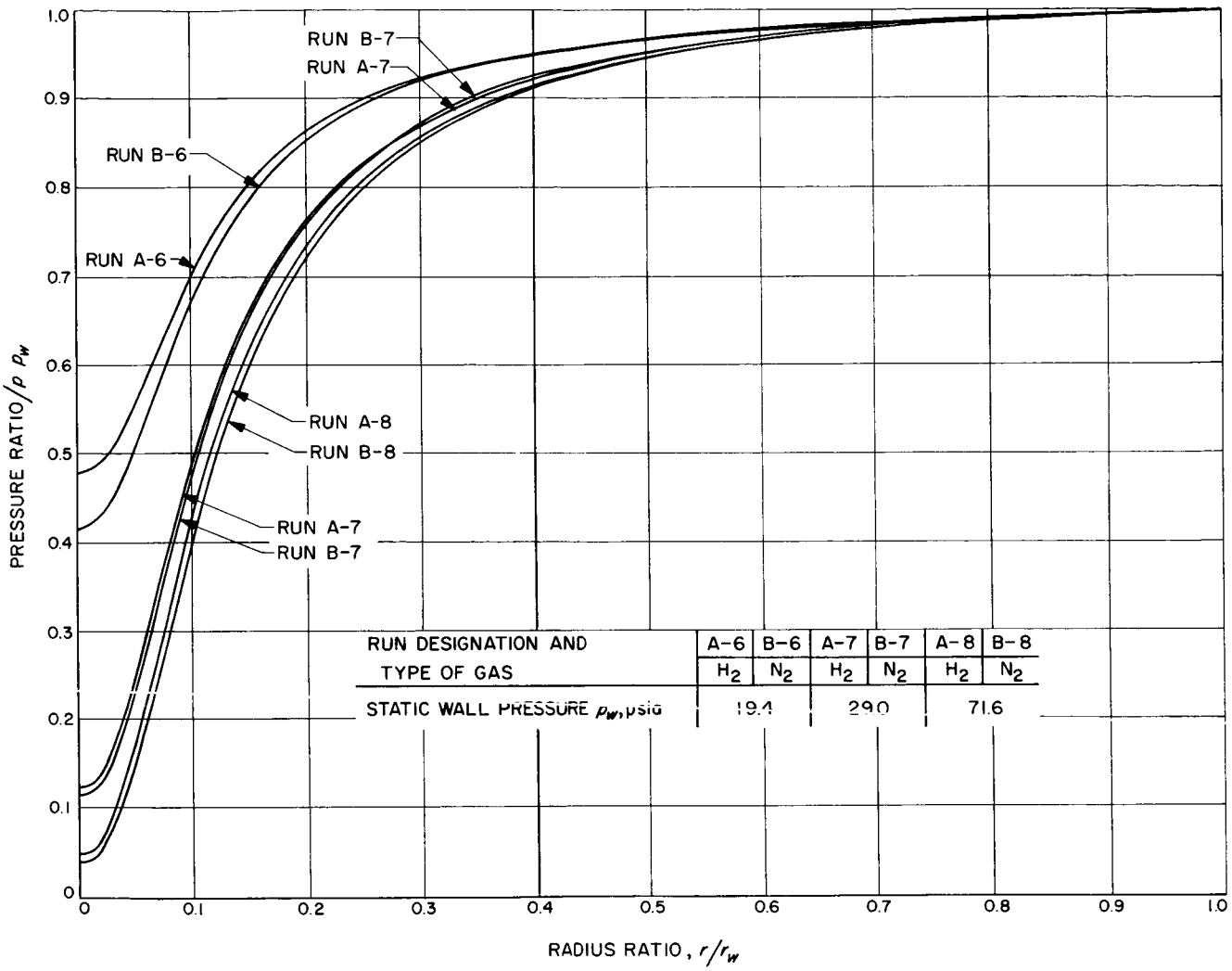

Fig. 6. Comparisons of pressure distributions between hydrogen and nitrogen run at equal values of static wall-pressure with a 0.010-in.-D wire stretched across vortex diameter

A-7 and B-7, for which the pressure distributions intersect at least twice.

It is also interesting to note that the ratios of radial Reynolds number entered in Table 3 for nitrogen to hydrogen, i.e.,

$$(Re_r)_B/(Re_r)_A = (\dot{m})_B(\mu)_A/(\dot{m})_A(\mu)_B$$

are approximately constant and not strongly dependent on p_w. Furthermore, these values agree favorably with values of the measured similarity parameter $(p_w)_A/(p_w)_B$ listed in Table 2(a). If it is assumed that $(p_w)_A = (p_w)_B$, $(T_w)_A = (T_w)_B$, and the driving-jet orifices are choked, it is easily demonstrated that the following relation exists by applying the continuity equation and the equation of state for a perfect gas to the flow through the vortex driving jets:

$$\frac{(\dot{m})_B}{(\dot{m})_A} = \left[\frac{(\mathcal{M})_B}{(\mathcal{M})_A}\right]^{1/2} \tag{25}$$

Mass flow-rate ratios for the various run pairs listed in Table 3 are found to agree with Eq. 25 to within 4% without making the minor corrections for slightly differing gas temperature. Equation 25 may also be obtained by setting $(\dot{m})_B(\mu)_A/(\dot{m})_A(\mu)_B$ equal to the right-hand side of Eq. 23, an expression derived for $(p_w)_A/(p_w)_B$.

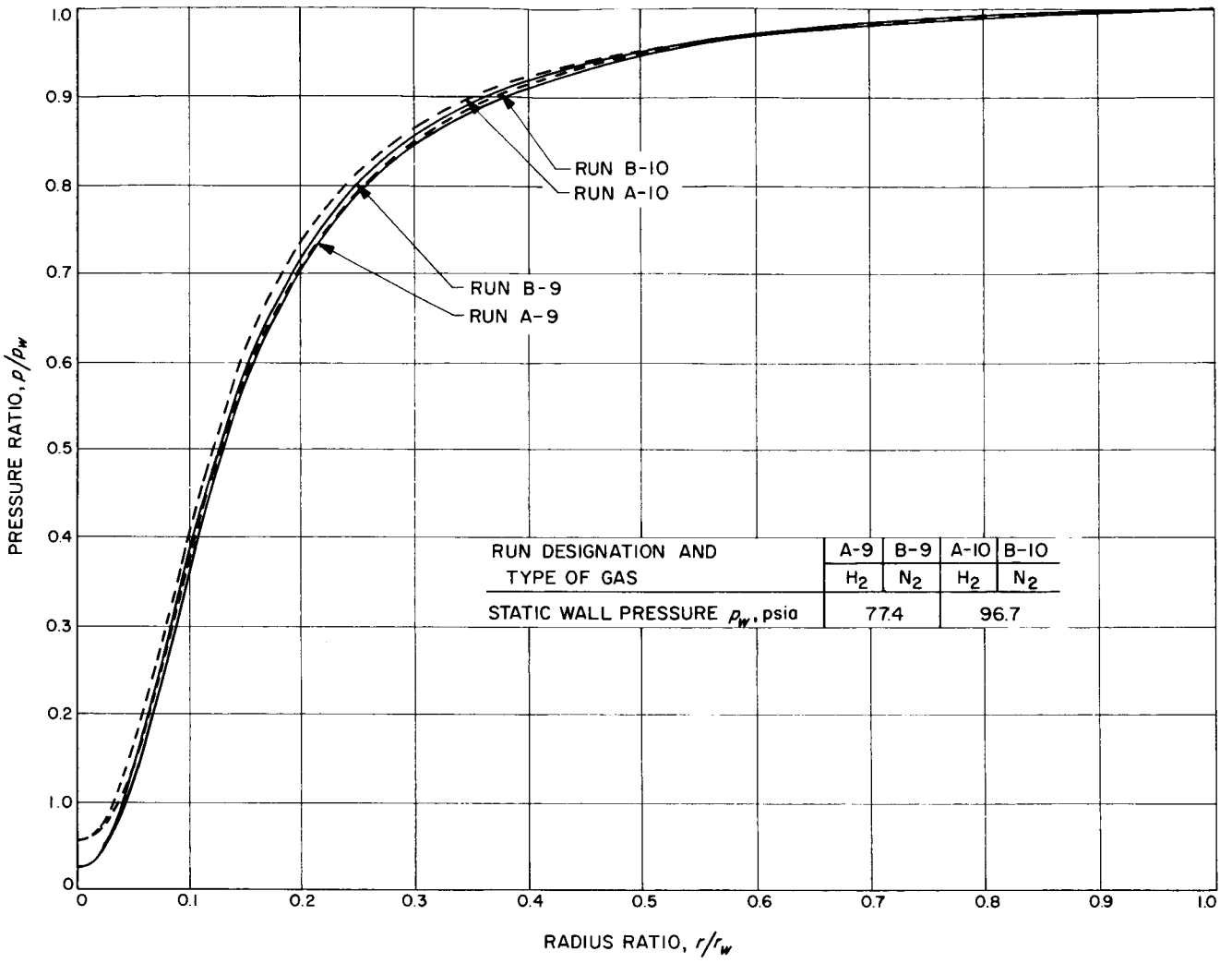

Fig. 7. Comparisons of pressure distributions between hydrogen and nitrogen run at equal values of static wall-pressure without wires stretched across vortex tube

V. DISCUSSION

Previous treatment of the boundary conditions for the vortex flow considered was incomplete, and certain consequences were avoided or not clearly stated. Present knowledge and understanding of vortex flows is not sufficient to take precise account of the boundary conditions; however, some of their pertinent features should be acknowledged. Since two-part solutions for pressure, velocity, and temperature are usually required, each in an appropriate domain of the radial coordinate, an internal boundary condition matching the two-part solutions is involved. Thus, in Ref. 1, solutions are matched at $r_o = d_o/2$ which, physically, is taken to be the exit-hole radius. At low values of Re_r, r_0 denotes the approximate radius of a viscous core in near solid-body rotation. Experiment indicates that the exit-hole radius r_o and the edge of the viscous core are related, but do not correspond

exactly, as most of the current theories postulate. The similarity model proposed here would require that (1) r_o/r_w remain constant from one vortex flow to another, and (2) that r_o/r_w be independent of the mass rate of flow $\dot{m}$. These statements are true only when the edge of the viscous core is related in some fixed way to the size of the exit hole. Such a unique relation is unknown.

Furthermore, the structure of a vortex core may depend on the shape of the exit hole and the magnitude of the ambient or discharge pressure, if the latter is greater than the static pressure at the vortex centerline. In these experiments, the entire vortex exit-hole configuration, including the axial position of the center plug shown in Fig. 2, was held constant.

The boundary conditions at the periphery of the vortex flow field, which, for purposes of discussion, may be considered as the edge of the boundary layer on the cylindrical wall, are intimately related to the manner and position of fluid injection. Prescribed geometric similarity of injection slits or jet orifices (based on a linear dimension) is not necessarily compatible with fluid boundary conditions at the vortex periphery. Again, this problem did not arise here because a single, unaltered device was used in the experiments. Aside from questions concerning the interaction between the cylindrical-wall boundary layer, the incoming jets or sheets of fluid, and the vortex flow field, one would have to consider the relative roughness of the vortex walls and the possibility of the fluid injection system choking.

If the driving-jet orifices become choked, the static pressure at the exit of the jets is not necessarily equal to the static pressure at the cylindrical wall. For constant-diameter jet-tubes, the exit Mach number is limited to unity; however, the fluid could further accelerate by expansion while mixing with the vortex flow. One assumption utilized in the similarity model was that Re_r and Re_t were directly proportional, or very nearly so. In Ref. 4, it was found that Re_t varied with Re_r approximately to the 1.09 power for subsonic jets. However, that result could be incorrect for application here if the jet orifices were choked during some of the experimental runs. Accordingly, it became desirable to know if the jet orifices were choked and, if so, to what extent this fact would alter the assumption of proportionality between Re_r and Re_t. In particular, it then became desirable to know if, for example, run A-1 were operating with choked jet-orifices, whereas run B-1 were not, and similarly for run 2. The injection system in the device employed here consisted of small, constant-diameter tubes having lengths approximately 130 times their diameter.

Assuming adiabatic flow with friction in the driving-jet tubes, dimensionless mass-flow rates were computed and compared with standard Fanno results. The result is shown in Fig. 8, where the parameter $4fL/D$ refers to the friction parameter for the jet tubes and not to wall friction in the vortex. The choking line is determined by the locus of the critical pressure ratio that depends on the magnitude of $4fL/D$ and, alternatively, the dimensionless mass rate of flow. All of the similarity runs are labeled, as shown in Fig. 8; unlabeled points refer to runs listed in Table 3. It is thus determined that the critical pressure ratio for these jet tubes p_w/p_{tm} is approximately 0.33, which corresponds to a dimensionless mass-flow rate of approximately 0.43 and $2<4fL/D<3$. From these results, it appears that all runs were made with less than critical pressure ratio and the jet tubes were choked in each case. Thus, the Mach number and, to good approximation, the velocity at the exit of the jet tubes were constant in these

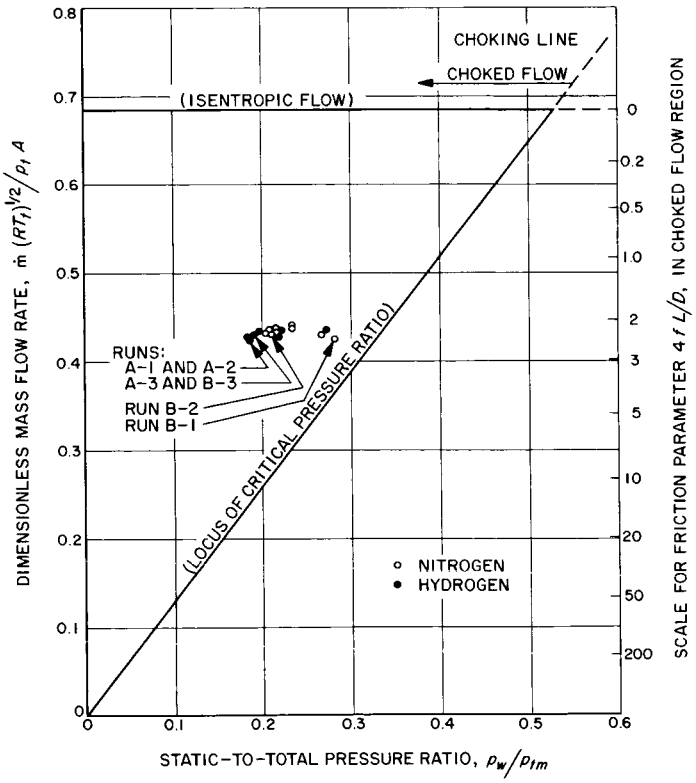

Fig. 8. Determination of choked flow condition for vortex driving jets; comparison of experimental data with standard Fanno results

experiments. The ratio of the tube exit pressure p_j to the wall pressure p_w was in the range $1.2 < p_j/p_w < 1.8$.

The relationship between Re_t and Re_r was reappraised by extending the case presented in Ref. 4 to the more general case of $\rho_j \neq \rho_w$ or $p_j \neq p_w$ in Ref. 8, where it was assumed that the gas expanded isentropically from p_j to p_w. The result of that investigation indicated that for the rather low ratios of p_j/p_w obtained in these experiments the effect of choked jet-orifices was to render the assumption of direct proportionality between Re_t and Re_r even more accurate than for the case of subsonic jet orifices.

The two-dimensional similarity model proposed and tested here is obviously deficient in that it fails to consider the effects of turbulence and the existence of axial velocities. Axial velocity near the vortex centerline is probably of the same order of magnitude as the tangential component. Reliable experimental information on both turbulence and axial velocities in vortex flows is so scarce that meaningful models including their effects cannot be presently formulated. As was stated earlier, this does not justify excluding their effects from an analysis. Although nothing concerning the axial velocity is known in these experiments, an approximate idea of the magnitudes of the radial and tangential components may be obtained by comparing Reynolds numbers at the cylindrical wall. The ratio of Reynolds numbers Re_r/Re_t, which is approximately equal to $|u_w|/v_w$, is listed for the various runs in Table 2(b). At the wall, the inferred tangential components are typically several orders of magnitude larger than the radial components. The absolute value of u is indicated since, by convention, it is negative in this application.

A deeper significance for $|u|/v$ in vortex flows is presented and discussed in Ref. 9. It is suggested that, whereas Re_r is the controlling parameter in a two-dimensional, laminar vortex flow, Re_r has relatively weak influence in a turbulent vortex flow that is, rather, controlled by the $|u|/v$ ratio. The physical arguments put forward in Ref. 9 are further reinforced by considerable analytical and experimental work. It is further suggested that the $|u|/v$ ratio is essentially independent of the mass flow rate (and thus Re_r) for vortex devices having a fixed injection configuration and that $|u|/v$ can be changed only by changing $\dot{m}$ independently of the injection velocity. This requires variable injection configuration, although in some cases changes can be obtained in devices having fixed injection configuration in which the flow is choked. The experimental results reported in Ref. 9 were accomplished using a significantly different configuration than used here, and the vortexes generated were much weaker than obtained here, as judged by the ratio v_{max}/v_w. Therefore, those results should not be considered completely general.

It is of interest to point out that the $|u|/v$ ratio bears significance also in laminar vortex flows, as clearly shown by Lewellen (Ref. 10), and even in certain inviscid vortex flows, as shown by Long (Ref. 11). As can be easily shown, the expansion parameter used by Lewellen to obtain a series solution for the incompressible, axisymmetric Navier-Stokes equations is numerically equivalent to the Rossby number used by Long, although the definitions and the applications are quite different. The Rossby number Ro is defined as the ratio of the inertia forces to the Coriolis forces in a rotating fluid. Since some form of Rossby number appears to have significance in a wide variety of vortex flows, it is of interest to examine the present experimental data to determine approximate magnitude of the Rossby number and its possible influence on the results. Although the Rossby number or a ratio such as $|u_w|/v_w$ does not appear explicitly in the similarity model proposed here, its presence is implied through the assumed proportionality between Re_t and Re_r, as will now be demonstrated. Thus, the Rossby number may be considered as a supplementary similarity parameter.

The form of Rossby number used by Lewellen (Ref. 10), is equivalent to $Q/2\pi r_o \Gamma_\infty$ where Q is the volume flow rate, r_o is a reference radial dimension, and Γ_∞ the circulation vr far from the vortex axis. Applied at the cylindrical wall of the vortex, this formulation for Ro becomes $Q/2\pi v_w r_w^2 = \dot{m}/2\pi\rho_w v_w r_w^2$. If the last expression for Rossby number is multiplied by r_w/L, it is at once seen that $r_w Ro/L = Re_r/Re_t = |u_w|/v_w$ so that the values of $|u_w|v_w$ listed in Table 2(b) may be construed as a form of Rossby number. Thus, the values of $|u_w|/v_w$ in this experiment are of order 10^{-3}; the value of Rossby number in the sense of Lewellen and Long is $10^{-3} \times L/r_w$ or approximately 10^{-2}. With the exception of Run B-1, which appears to have a low value of Re_r, as judged by its Re_r/Re_t ratio, the values of $|u_w|/v_w$ for the similarity runs differ by only 11% over a wide range of Re_r demonstrating the approximate proportionality between Re_t and Re_r (or between $|u_w|$ and v_w) indicated in Refs. 4, 8 and 9. In contrast to the remarks and some of the experimental results presented in Ref. 9, however, these results show that significant changes in the vortex flow field did occur when Re_r or $\dot{m}$ was varied at approximately constant $|u_w|/v_w$ (see pressure and Mach number distributions, Figs. 3, 4 and 5).

In applying the similarity model to the experiment presented here, it might appear that the results depend primarily on just one parameter, $Re_r = \dot{m}/2\pi\mu L$. Since Re_r and Re_t are almost directly proportional, this would be true if M_w was also related to Re_r in such a way that the relationship would be invariant to the type of gas used in a fixed vortex configuration. Although the data is insufficient, examination of the data presented in Table 2(b) yields some evidence that this may be true. Such a relationship between Re_r and M_w can be demonstrated at present only by resorting to empirical data, or by making assumptions concerning the relationship between $\dot{m}$ and p_w in a given apparatus. Therefore, the relationship cannot be considered general and should be disregarded especially in considering the case of similarity in two or more vortex tubes, differing in dimensional scale.

For purposes of comparison in this experiment, assume that a definite relationship between Re_r and M_w does exist, and that it does not depend on which of the gases, nitrogen or hydrogen, was used. Following the proposed similarity model for a fixed vortex configuration exhausting to atmospheric pressure, dynamic flow similarity merely requires setting of the mass flow rates proportional to the viscosity ratio, or $\dot{m}_A/\dot{m}_B = \mu_A/\mu_B$. The results listed in Table 2(a) show this to be approximately realized. However, the data in Figs. 3 and 4 do not illustrate flow similarity, clearly showing that one parameter is not sufficient for achieving similarity; hence the proposed model is too restrictive. Since Re_r is the only independent flow variable (because it is directly related to the inlet stagnation pressure for fixed vortex configuration), and the only one directly measurable, it appears that the problem of producing dynamically similar vortex flows for known reasons is indeed a formidable one.

The failure of the theoretical similarity model as tested by experiment is not difficult to understand in view of its very restrictive nature. However, the results of the experimental tests performed at constant values of static wall pressure, which yielded relatively better similarity in end-wall static-pressure distributions, is neither easy to understand nor to explain. It would appear that the molecular transport properties (such as viscosity and thermal conductivity) of the gases employed were either not involved or of negligible importance. For a vortex of fixed configuration, it would appear that the nature of the vortex flow field may be controlled by turbulent transport properties which, in turn, may be controlled by mass rate of flow and/or the size and shape of the injection system and the particular apparatus employed. Alternatively, one might say that for diatomic (or monatomic) gases the vortex flow field is controlled merely by static pressure ratio across the device, and possibly the absolute level of the ambient or atmospheric discharge pressure. It is unfortunate that additional experiments of this nature were not performed using several other gases, such as helium, argon, carbon dioxide, or some of the freons. Such tests would have given additional information concerning the effects of transport properties, molecular weight, Prandtl number, etc.

It is likely that dynamic similarity in jet-driven vortex flows is strongly related to the particular vortex configuration employed, not only to the aspect ratio and relative exit-hole size but, perhaps as importantly, the arrangement and number of the driving-jet orifices or slots. Experimental data presented in Ref. 9 indicate some of the results of widely varying injection configuration which, as was discussed in that reference, may contribute to or control the scale of turbulence that occurs. In addition, the absolute diameter of the device is important, since the frictional effects of the cylindrical and end-walls vary with this dimension, as shown in Ref. 4 and more completely in Ref. 12. Thus, the problems of geometric scaling are indeed difficult, and it is possible that dynamic flow similarity in two separate vortex devices cannot be achieved under conditions of exact geometric similarity. This, in turn, is no doubt due in large measure to the difficulty of achieving similarity in boundary conditions, since exact similarity in the boundary conditions is not necessarily guaranteed by exact geometric similarity.

VI. SUMMARY AND CONCLUSIONS

A similarity model for laminar, compressible, viscous, two-dimensional vortex flow has been developed and the results of a limited experimental program designed to test its effectiveness have been presented. Two gases, nitrogen and hydrogen, were tested at conditions prescribed by the model in identically the same vortex apparatus in three separate experiments. Similarity was judged on the basis of the non-dimensional distributions of static pressure measured on the solid end-wall, and the tangential Mach number distributions obtained from these pressure distributions. Some of the limitations and drawbacks of the model are discussed.

It is concluded that this similarity model is generally inadequate, even as applied to the simple experiment described. Although it was found possible to produce similar static-pressure distributions in nitrogen and hydrogen, the conditions of this occurrence were not found to be governed by the requirements of the model. Similarity was achieved by adjusting the mass flow rate, in either case, to a value sufficient to obtain what appeared to be an approximate limiting-pressure distribution for this vortex tube; i.e., the condition for which relatively large increases in the mass flow rate affect the pressure distribution only slightly and, then, only in a region near the vortex axis. Since an experimental application of the model depends primarily on just one, measurable independent parameter, the mass flow rate per unit length of vortex tube, it would appear that only detailed empirical knowledge of vortex flow structure will enable an investigator to set forth rules for dynamic flow similarity. One parameter is not sufficient for achieving similarity.

Some additional test results, which were obtained in a different set of experiments but using the identical apparatus, have also been presented to indicate a method by which more satisfactory similarity results between the two gases was achieved as compared with the previous results. That method was simply to operate the vortex apparatus with each of the gases at the same value of static wall pressure p_w.

NOMENCLATURE

A	total cross-sectional area of driving jets
c_p	specific heat of gas
d_o	diameter of exit hole
D	diameter of vortex tube
f	average friction coefficient for driving jet-orifices
k	thermal conductivity of gas
L	length of vortex tube
$\dot{m}$	mass flow rate
$\mathcal{M}$	molecular weight of gas
M	tangential mach number
p	pressure
Pr	Prandtl number ($= \mu c_p/k$)
q	dynamic pressure ($= \rho v^2/2$)
Re_r	radial Reynolds number ($= \dot{m}/2\pi\mu L$)
$Re_{r,e}$	effective radial Reynolds number
Re_t	peripheral tangential Reynolds number ($= \rho_w v_w D/2\mu$)
R	gas constant
r,θ,z	radial, angular and axial polar coordinates, respectively
T	temperature
u,v,w	radial, tangential and axial velocity components, respectively
γ	ratio of gas specific heats
μ	dynamic (molecular) viscosity
ρ	gas density

Subscripts

A,B	refers to hydrogen and nitrogen, respectively
a	ambient or atmospheric condition
j	refers to conditions at the exit of the driving jet-orifices
m	manifold or plenum condition
t	total or stagnation condition
w	refers to cylindrical wall (edge of free stream)
$*$	refers to parameter normalized with respect to its value at cylindrical wall

REFERENCES

1. Einstein, H. A., and Li, H. L., "Steady Vortex Flow in a Real Fluid," *Proceedings of the Heat Transfer and Fluid Mechanics Institute,* Stanford University, June 1951, pp. 33–43.

2. Keyes, J. J., Jr., *An Experimental Study of Flow and Separation in Vortex Tubes with Application to Gaseous Fission Heating,* ARS Paper No. 1516-60, ARS 15th Annual Meeting, Washington, D.C., December 1960.

3. Roschke, E. J., "An Examination of Vortex Strength in a Compressible Viscous Vortex," *Space Programs Summary 37-20, Vol. IV,* Jet Propulsion Laboratory, Pasadena, California, April 30, 1963, pp. 73–76.

4. Roschke, E. J., "Some Gross Effects of Cylindrical Wall-Friction and End-Wall Boundary Layer Flow on Confined Vortex Flows," *Space Programs Summary 37-21, Vol. IV,* Jet Propulsion Laboratory, Pasadena, California, June 30, 1963, pp. 102–108.

5. Rosenzweig, M. L., *Summary of Research in the Field of Advanced Nuclear Propulsion,* Propulsion Research Program, Semiannual Technical Report, Report No. TDR-930(2210-140TR-1), Laboratories Division, Aerospace Corporation, March 1962.

6. Ragsdale, R. G., *Applicability of Mixing Length Theory to a Turbulent Vortex System,* NASA TN D-1051, August 1961.

7. Pivirotto, T. J., "Binary Diffusion in a Compressible, Three-Dimensional Turbulent Vortex," *Space Programs Summary 37-18, Vol. IV,* Jet Propulsion Laboratory, Pasadena, California, December 31, 1962, pp. 129–132.

8. Roschke, E. J., "Additional Remarks on Reynolds Number Relations in Vortex Flows," *Space Programs Summary 37-31, Vol. IV,* Jet Propulsion Laboratory, Pasadena, California, February 28, 1965, pp. 174–178.

9. Craig, R. T., Davis, W. C., Coerdt, R. J., Donaldson, C. duP., McCune, J. E., Williamson, G. G., and Ostrach, S., *Research and Development in a Vortex MHD Power Generator,* Final Report, No. ER-4737, TAPCO Division, Thompson Ramo Wooldridge, Inc., December 1961.

10. Lewellen, W. S., "A Solution for Three-Dimensional Vortex Flows with Strong Circulation," *Journal of Fluid Mechanics,* Vol. 14, Part 3, November 1962, pp. 420–432.

11. Long, R. R., "Sources and Sinks at the Axis of a Rotating Liquid," *Quarterly Journal of Mechanics and Applied Mathematics,* Vol. 9, Part 4, pp. 385–393, 1956.

12. McLafferty, G. H., *Friction Coefficient Between a Rotating Gas and the Surface of a Containing Tube,* Report No. M-1686-6, United Aircrapt Corporation, Research Laboratories, September 1960.